

## **BRAF V600E mutation correlates with suppressive tumor immune microenvironment and reduced disease-free survival in Langerhans cell histiocytosis**

Kaixuan Zeng<sup>a</sup>, Zhe Wang<sup>a</sup>, Koichi Ohshima<sup>b</sup>, Yixiong Liu<sup>a</sup>, Weichen Zhang<sup>a</sup>, Lu Wang<sup>a</sup>, Linni Fan<sup>a</sup>, Mingyang Li<sup>a</sup>, Xia Li<sup>a</sup>, Yingmei Wang<sup>a</sup>, Zhou Yu<sup>a</sup>, Qingguo Yan<sup>a</sup>, Shuangping Guo<sup>a</sup>, Jie Wei<sup>a</sup>, and Ying Guo<sup>a</sup>

<sup>a</sup>Department of Pathology, State Key Laboratory of Cancer Biology, Xijing Hospital, Fourth Military Medical University, Xi'an, Shaanxi, People's Republic of China; <sup>b</sup>Department of Pathology, School of Medicine, Kurume University, Kurume, Fukuoka, Japan

### **ABSTRACT**

Langerhans cell histiocytosis (LCH) is a neoplasm of myeloid origin characterized by a clonal proliferation of CD1a<sup>+</sup>/CD207<sup>+</sup> dendritic cells. Recurrent *BRAF* V600E mutation has been reported in LCH. In the present report, we confirm the feasibility of the high-specificity monoclonal antibody VE1 for detecting *BRAF* V600E mutation in 36/97 (37.1%) retrospectively enrolled patients with LCH; concordant immunohistochemistry and Sanger sequencing results were seen in 94.8% of cases. We then assessed the tumor immune microenvironment status in LCH, and found that the GATA binding protein 3 (GATA3)<sup>+</sup>/T-bet<sup>+</sup> ratio could distinguish between clinical multi-system/single-system (SS) multifocal and SS unifocal LCH. Notably, we found that *BRAF* V600E mutation is significantly correlated with increased programmed cell death 1 ligand 1 (PDL1) expression and forkhead box protein 3 (FOXP3)<sup>+</sup> regulatory T cells ( $p < 0.001, 0.009$ , respectively). Moreover, Cox multivariate survival analysis showed that *BRAF* V600E mutation and PDL1 were independent prognostic factors of poor disease-free survival (DFS) in LCH (hazard ratio [HR] = 2.38, 95% confidence interval [CI] 1.02–5.56,  $p = 0.044$ ; HR = 3.06, 95%CI 1.14–7.14,  $p = 0.025$ , respectively), and the superiority of PDL1 in sensitivity and specificity as biomarker for DFS in LCH was demonstrated by receiver operator characteristic (ROC) curves when compared with *BRAF* V600E and risk category. Collectively, this study identifies for the first time relationship between *BRAF* V600E mutation and a suppressive tumor immune microenvironment in LCH, resulting in disruption of host–tumor immune surveillance, which is DFS. Our findings may provide a rationale for combining immunotherapy and *BRAF*-targeted therapy for treating patients with *BRAF* V600E mutant LCH.

**Abbreviations:** DFS, disease-free survival; FOXP3, transcription factor forkhead box protein 3; GATA-3, GATA binding protein 3; IHC, immunohistochemistry; LCH, Langerhans cell histiocytosis; MS-LCH, multi-system langerhans cell histiocytosis; mut, mutated; PCR, polymerase chain reaction; PDL1, programmed cell death ligand 1; ROC, receiver operator characteristic; SS-LCH, single-system langerhans cell histiocytosis; T-bet, T-box expressed in T cells; TILs, tumor-infiltrating lymphocytes; Tregs, regulatory T cells; wt, wild-type

### **ARTICLE HISTORY**

Received 26 February 2016  
Revised 17 April 2016  
Accepted 27 April 2016

### **KEYWORDS**

*BRAF* V600E; immunotherapy; LCH; prognosis; targeted therapy; tumor immune microenvironment; VE1


## **Introduction**

Langerhans cell histiocytosis (LCH), also known as histiocytosis X, combines in one nosological category a group of diseases that have widely disparate clinical manifestations but are all characterized by the accumulation of proliferating cells with surface markers and ultrastructural features similar to cutaneous Langerhans cells (LCs).<sup>1</sup> LCH occurs predominantly in children but also occurs in adults; the ratio of male to female patients is approximately 2:1.<sup>2</sup> Lesions are most common in the bone (eosinophilic granuloma) and skin, but may occur in other organs. The clinical course varies from lesions that spontaneously resolve, to chronic disease, or it can be disseminated and life-threatening.<sup>3</sup> Based on the number of diseased organs and systems, LCH can be divided into two types: single-system

(SS-LCH) and multi-system (MS-LCH). SS-LCH can also be divided into SS unifocal LCH and SS multifocal LCH.

The classification of LCH as either reactive or neoplastic disease had not been resolved until the recent detection of activating *BRAF* mutations in approximately half of LCH lesions,<sup>4</sup> and the subsequent meta-review involving 653 patient samples that determined an overall frequency of 48.5% for the *BRAF* V600E point mutation in LCH.<sup>5</sup> favored LCH as a neoplastic disease. Although cancer has been considered a progression of genetic mutations in an aberrant tissue mass, tumors are increasingly viewed as tissues functionally interconnected with the surrounding microenvironment.<sup>6</sup> Due to its rarity and diverse nature, relatively little is known of the contribution of the LCH

**CONTACT** Ying Guo  [guoying@fmmu.edu.cn](mailto:guoying@fmmu.edu.cn)  Associate Professor, Department of Pathology, Xijing Hospital, Preclinical School, Fourth Military Medical University, Changlexi Street No.169, Xi'an City, Shaanxi province, People's Republic of China.

 Supplemental data for this article can be accessed on the [publisher's website](#).

Published with license by Taylor & Francis Group, LLC © Kaixuan Zeng, Zhe Wang, Koichi Ohshima, Yixiong Liu, Weichen Zhang, Lu Wang, Linni Fan, Mingyang Li, Xia Li, Yingmei Wang, Zhou Yu, Qingguo Yan, Shuangping Guo, Jie Wei, and Ying Guo.

This is an Open Access article distributed under the terms of the Creative Commons Attribution-Non-Commercial License (<http://creativecommons.org/licenses/by-nc/3.0/>), which permits unrestricted non-commercial use, distribution, and reproduction in any medium, provided the original work is properly cited. The moral rights of the named author(s) have been asserted.

microenvironment to disease pathogenesis. In this context, and even if our current understanding of the tumor immune microenvironment in LCH remains limited when compared with other cancers, several data suggest that exploring the immune system is an interesting strategy. Immune cells such as T cells, regulatory T cells (Tregs), T helper (Th)17 cells, and macrophages are present in clinical LCH samples.<sup>7,8</sup> Recently, studies have shown that the *BRAF* V600E protein mutation is associated with immunosuppressive mechanisms in melanoma and papillary thyroid cancer, such as forkhead box protein 3 (FOXP3) and programmed cell death 1 ligand 1 (PDL1) expression.<sup>9,10</sup> It has been indicated that *BRAF* mutation leads to disruption of endogenous host immune surveillance and the promotion of tumor immune escape. Whether these mechanisms of immune suppression occur analogously in *BRAF* V600E LCH has not been studied.

In the present study, we assessed the tumor immune microenvironment status in LCH and investigated the relationship between *BRAF* mutation status and known strategies of tumor-mediated immune suppression, and further analyzed their relation to clinicopathological or prognostic relevance in archival material from 97 relatively well-defined cases of LCH.

## Results

### Clinical information

The clinical characteristics and outcome of 97 LCH patients are summarized in Tables 1 and S1, including 65 children (< 18 y old) and 32 adult patients (≥ 18 y old). The average and median age of the overall cohort was 16.6 and 10 y old (range 1–63), respectively. And the median age of children and adults was 6 and 37.5 y old, respectively. A total of 89 patients (91.8%) had a single-system involvement while eight patients (8.2%) had multisystem diseases. Ninety-one cases belonged to low risk LCH, six cases belonged to high risk LCH.

**Table 1.** The clinical characteristics of LCH patients (n = 97).

Variable	Total (n = 97)	Percentage
Gender		
Male	63	64.9%
Female	34	35.1%
Age		
< 18	65	67%
≥ 18	32	33%
Biopsy site		
Bone	83	77.6%
Lymph node	13	12.1%
Liver	5	4.7%
Skin	3	2.8%
Lung	2	1.9%
Spleen	1	0.9%
Risk category		
Low	91	93.9%
High	6	6.1%
Clinical stage		
SS	89	91.8%
MS	8	8.2%

SS, single-system langerhans cell histiocytosis; MS, multi-system langerhans cell histiocytosis.

At the end of the follow-up period, 93 patients were still alive and four had died of the disease. Our data show that the most frequently documented management option was resection, followed by chemotherapy, and radiotherapy.

### Mutant protein and *BRAF* V600E mutation in LCH lesions

The presence or absence of the *BRAF* V600E mutation was determined in 97 lesions by Sanger sequencing and VE1 immunohistochemistry (IHC) (Table 2). DNA isolation and PCR proved successful in all cases. Similarly, IHC was informative in all sections of histologically proven histiocytic proliferations. Sanger sequencing demonstrated *BRAF* mutation (the mutation sites were all in p.V600E) in 31/97 samples (32%), whereas IHC analysis detected mutant protein in 36/97 cases (37.1%) (Fig. 1). In five cases, the *BRAF* V600E alteration was detected by IHC only and not by Sanger sequencing. Concordant Sanger sequencing and IHC results were seen in 94.8% of cases.

### *BRAF* V600E mutation is significantly correlated to increased PDL1 expression and FOXP3+ Tregs in LCH tissues

We assessed the relationship between *BRAF* mutation (*BRAF*-mut) and the tumor immune microenvironment. VE1, PDL1, and FOXP3+ Treg staining was performed on the 97 LCH tissues by IHC, using the H-score as a semiquantitative approach. The mean PDL1 expression and FOXP3+ Tregs were significantly higher in *BRAF*-mut patients as compared with patients with wild-type *BRAF* (*BRAF*-wt) (141.29 versus 62.81,  $p < 0.001$ ; 43.55 versus 21.59,  $p = 0.009$ , respectively) (Fig. 2A and B). However, no significant differences in GATA binding protein 3 (GATA3)+/T-bet+ (G/T) ratio were observed between *BRAF*-mut and *BRAF*-wt patients (6.58 versus 6.35,  $p = 0.325$ ) (Fig. 2C). Strong and medium correlation was observed between VE1 H-score and PDL1 ( $r = 0.635$ ,  $p < 0.001$ ) and FOXP3 H-scores ( $r = 0.429$ ,  $p < 0.001$ ), respectively (Fig. 2D and E). These results indicate that *BRAF* mutation lead to increased PDL1 expression and FOXP3+ Tregs and could be a more intuitive presentation of two representative LCH cases (Fig. 3). Recently, *MAP2K1* mutation has been reported in *BRAF*-wt cases.<sup>11</sup> We also detected *MAP2K1* mutation using Sanger sequencing. Among the 97 LCH samples, 17 cases (17.5%) harbored a *MAP2K1* mutation which was mutually exclusive with *BRAF* mutation (Table S1). No statistically significant association was found between *MAP2K1* mutation status and PDL1, FOXP3+ Treg, or (G/T) ratio (all  $p > 0.05$ ) (Fig. S1).

**Table 2.** Results of *BRAF* V600E mutation testing using Sanger sequencing and IHC in 97 LCH cases.

Sanger Sequencing	Immunohistochemistry		Total
	VE1-negative	VE1-positive	
BRAFV600E-wt	61	5	66
BRAFV600E-mut	0	31	31
Total	61	36	97

wt = wild-type; mut = mutated.

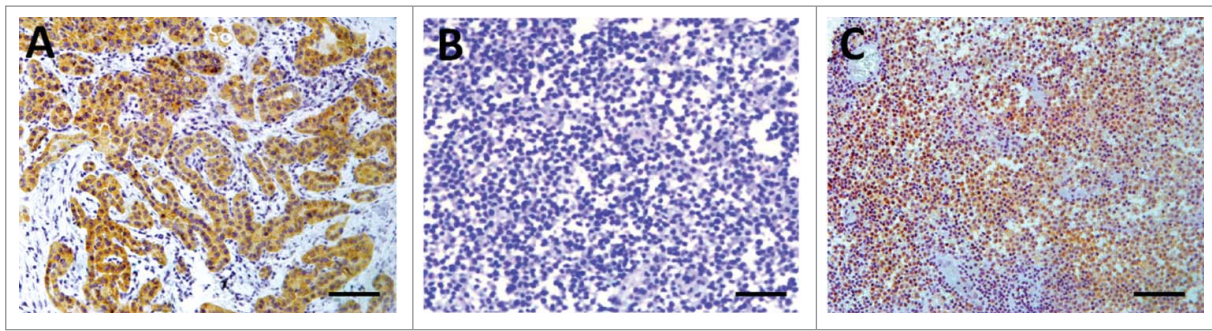


**Figure 1.** Immunohistochemistry for VE1. (A) Papillary thyroid carcinoma with *BRAF* V600E mutation (positive control), diffusely strong cytoplasmic staining. (B) Phosphate buffered saline was used instead of VE1 (negative control). (C) One representative LCH case with *BRAF* V600E mutation, diffusely strong cytoplasmic staining. Original magnification  $\times 20$ , scale bar =  $50 \mu\text{m}$ .

### The G/T ratio of tumor-infiltrating lymphoid cells distinguishes between clinical MS/SS multifocal LCH and SS unifocal LCH

T-bet and GATA3 are two transcription factors that determine Th cell differentiation into Th1 or Th2, respectively. To determine the possible association between Th1/Th2 differentiation and disease progression, we enumerated by double IHC the GATA3<sup>+</sup> and T-bet<sup>+</sup> infiltrating lymphoid cell LCH samples from 97 patients (Fig. 4A). GATA3 and T-bet were both expressed in the nuclei of tumor-infiltrating lymphoid cells. As the amounts of lymphoid cells in the tumor varied among samples, we calculated the percentage of positive lymphoid cells for each patient, and found that the percentage of GATA3<sup>+</sup> cells was significantly higher than that of T-bet<sup>+</sup> ( $p < 0.001$ ) (Fig. 4B). However, the percentage of GATA3<sup>+</sup> cells varied among the samples (Fig. 4B). To verify possible quantitative differences among samples, we calculated the G/T ratio for

each patient, and the median G/T ratio was 3.2 (Fig. 4C). Indeed, the G/T ratio did not correlate with sex, age, extent of lesion, and clinical risk status (all  $p > 0.05$ ) (Table 3). The Cox regression model also showed no significant correlation between the G/T ratio and disease-free survival (DFS) (hazard ratio [HR] = 1.06; 95% confidence interval [CI] 0.48–2.34;  $p = 0.88$ ) (Table 4). However, a significant correlation between the G/T ratio and extent of lesion was detected when SS LCH was divided into SS unifocal LCH and SS multifocal LCH. The mean G/T ratio values were significantly higher in MS LCH and SS multifocal LCH as compared with SS unifocal LCH (14.63 versus 3.85,  $p = 0.004$ ; 8.39 versus 3.85,  $p = 0.031$ , respectively) (Fig. 4D). In addition, GATA3 was more frequently expressed in MS LCH than in SS multifocal LCH, although the association was not statistically significant (14.63 versus 8.39,  $p = 0.183$ ) (Fig. 4D). No significant differences in VE1, PDL1, and FOXP3 H-score were observed between the three groups (all  $p > 0.05$ ) (Fig. 4E–G).

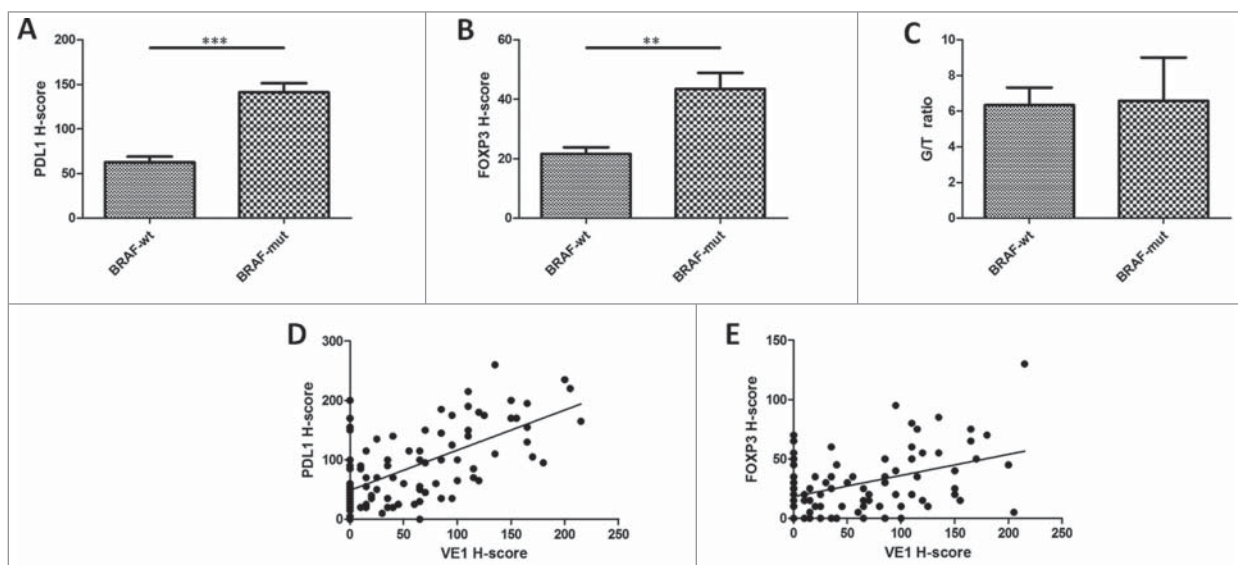


**Figure 2.** *BRAF* V600E mutation is significantly correlated with increased PDL1 and FOXP3 expression in LCH tissues ( $n = 97$ ). (A) Examination of PDL1 expression by IHC using the H-score. PDL1 expression was higher in BRAF-mut patients ( $n = 31$ ) as compared with BRAF-wt patients ( $n = 66$ ) ( $p < 0.001$ ). (B) Examination of FOXP3 expression by IHC using the H-score. FOXP3 expression was higher in BRAF-mut patients as compared with BRAF-wt patients ( $p = 0.009$ ). (C) No statistical difference between *BRAF* mutation status and G/T ratio ( $p = 0.325$ ). (D) Positive correlation between PDL1 and VE1 H-scores by IHC ( $p < 0.001$ , Pearson correlation = 0.635). (E) Positive correlation between FOXP3 and VE1 H-scores by IHC ( $p < 0.001$ , Pearson correlation = 0.429). wt = wild-type; mut = mutated; G/T ratio = GATA3<sup>+</sup>/T-bet<sup>+</sup> ratio. An unpaired *t*-test was used to calculate the two-sided *p*-values. \*\* $p < 0.01$ , \*\*\* $p < 0.001$ . Error bars represent standard deviation.



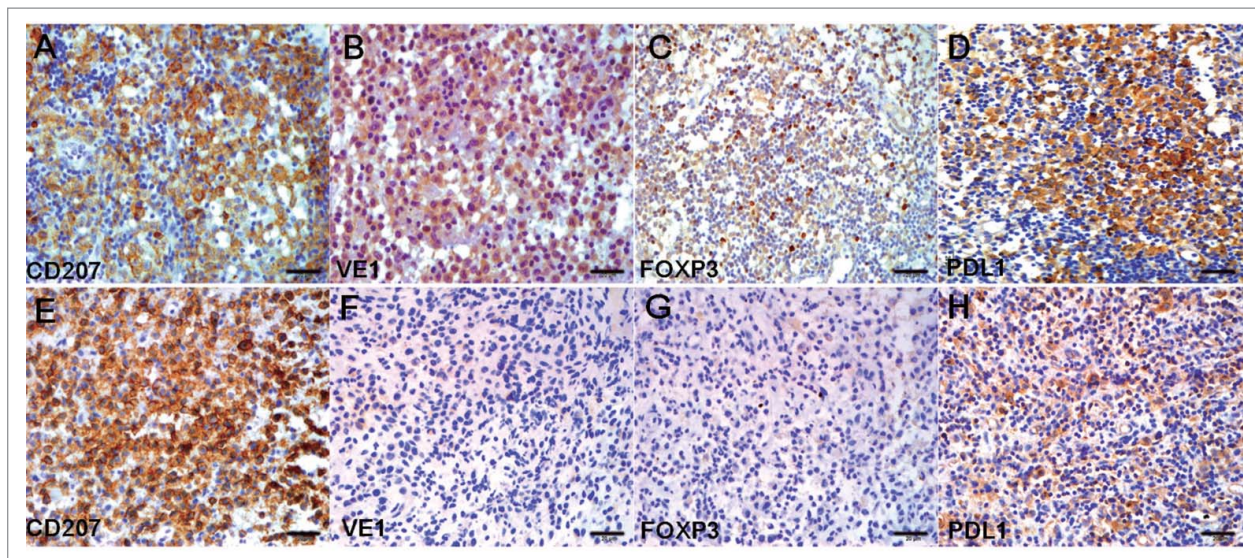


**Figure 3.** IHC for CD207, VE1, FOXP3, and PDL1 in serial sections of two representative LCH cases. (A–D) Case 1 had LCH with *BRAF* V600E mutation. (B) VE1, diffusely strong cytoplasmic staining; (C) FOXP3, moderate, focally strong nuclear staining; (D) PDL1, diffusely strong cell membrane and cytoplasmic staining. (E–H) Case 2 had LCH with wild-type *BRAF* V600E. (F) VE1, negative; (G) FOXP3, negative; (H) PDL1, weak cell membrane and cytoplasmic staining. Original magnification  $\times 40$ , scale bar = 20  $\mu\text{m}$ .

### ***BRAF* V600E mutation and PDL1 were independent negative prognostic factors for DFS in LCH**

The clinical significance of *BRAF* V600E mutation, FOXP3<sup>+</sup> Tregs, G/T ratio, and PDL1 were analyzed according to the categorical clinical variables sex, age, single-system versus multi-system, and high-risk versus low-risk clinical

assessment (Table 3). A significant difference was detected only between *BRAF* mutation status and age; *BRAF* V600E mutation occurred significantly more often in children patients than in adult patients ( $p = 0.015$ ). Given the very low number of patients who died (only four cases), the 5-y overall survival (OS) was 95.9%, which precluded any firm conclusion on OS. Kaplan–Meier DFS analysis of the 97

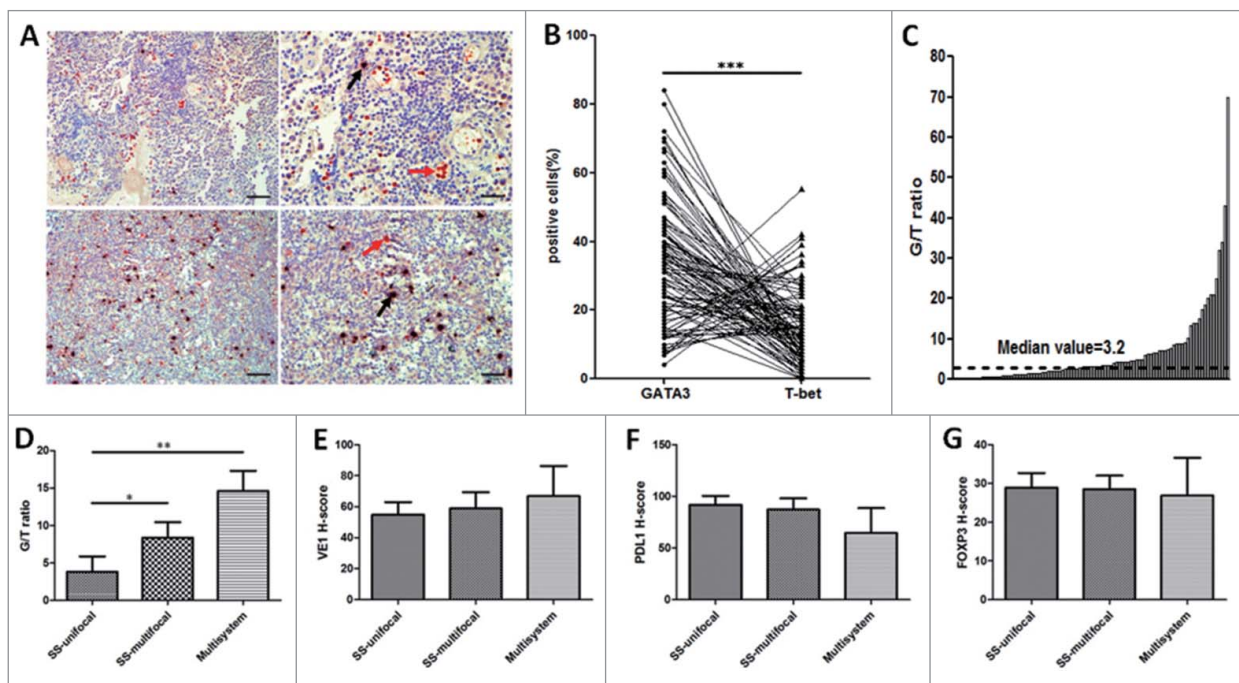


**Figure 4.** The G/T ratio in tumor-infiltrating lymphoid cells distinguishes between clinical MS/SS multifocal LCH and SS unifocal LCH. (A) Two representative double IHC analyses of lymphoid GATA3 and T-bet staining in LCH ( $n = 97$ ). The G/T ratio of case 1 (top)  $\geq 3.2$  (median value); the G/T ratio of case 2 (bottom)  $< 3.2$ . Red and black arrows indicate GATA3- and T-bet-positive cells in LCH, respectively. Original magnification  $\times 20$ , scale bar = 50  $\mu\text{m}$  (left); original magnification  $\times 40$ , scale bar = 20  $\mu\text{m}$  (right). (B) Percentage of GATA3<sup>+</sup> (circles) and T-bet<sup>+</sup> (triangles) lymphoid cells for each of the analyzed LCH samples ( $n = 97$ ). The values are significantly different as determined by paired two-tailed Student's *t*-test ( $p < 0.001$ ). (C) Waterfall plot of the G/T ratio for each LCH sample. The dashed line indicates G/T ratio = 3.2, which is the median value. (D) Mean G/T ratio of MS/SS multifocal versus SS unifocal LCH. SS multifocal ( $n = 36$ ) versus SS unifocal LCH ( $n = 53$ ) ( $P = 0.031$ ), MS ( $n = 8$ ) versus SS unifocal LCH ( $n = 53$ ) ( $P = 0.004$ ). (E–G) No significant differences in VE1, PDL1, or FOXP3 H-score were observed between the three groups (all  $p > 0.05$ ). An unpaired *t*-test was used to calculate the two-sided *p*-values. \* $p < 0.05$ , \*\* $p < 0.01$ , \*\*\* $p < 0.001$ . Error bars represent standard deviation.

**Table 3.** Correlation of LCH clinical characteristics with *BRAF* V600E mutation, FOXP3<sup>+</sup> Tregs, G/T ratio, and PDL1.

Variable	Total(n = 97)	<i>BRAF</i> mutated(n = 31)	<i>p</i> value	FOXP3 <sup>a</sup> high(n = 47)	<i>p</i> value	G/T ratio <sup>a</sup> high(n = 48)	<i>p</i> value	PDL1 <sup>b</sup> positive(n = 31)	<i>P</i> value
Gender									
M	63(64.9%)	22(34.9%)	0.394	27(42.9%)	0.144	30(47.6%)	0.681	17 (26.9%)	0.176
F	34(35.1%)	9(26.5%)		20(58.9%)		18(52.9%)		14(41.1%)	
Age									
<18	65(67%)	26(40%)	0.015*	35(53.8%)	0.087	29(44.6%)	0.193	25(38.4%)	0.065
≥18	32(33%)	5(15.6%)		12(37.5%)		19(59.3%)		6(18.7%)	
System									
SS	89(91.8%)	29(32.6%)	1.000	44(49.4%)	0.765	46(51.6%)	0.276	28(31.5%)	0.708
MS	8(8.2%)	2(25%)		3(37.5%)		2(25%)		3(37.5%)	
Risk									
Low	91(93.9%)	29(31.9%)	1.000	45(49.4%)	0.677	47(51.6%)	0.217	27(29.6%)	0.080
High	6(6.1%)	2(33.3%)		2(33.3%)		1(16.7%)		4(66.7%)	

M, male; F, female; SS, single-system LCH; MS, multi-system LCH.

\**p* < 0.05.

<sup>a</sup>Using median values as cutoff, <sup>b</sup>Staining intensity ≥ 2 in >5% of LCH cells.

cases revealed a correlation between *BRAF* mutation and positive PDL1 expression and shorter DFS (*p* = 0.01, 0.004, respectively) (Fig. 5). The factors that affected DFS in univariate analyses included system, risk category, *BRAF* mutation status, FOXP3<sup>+</sup> Tregs, and PDL1 (all *p* < 0.05) (Table 4). Age at diagnosis, sex, and G/T ratio did not have a statistically significant effect on DFS.

In addition, to obtain a more precise combined analysis of all the factors and to control for confounding factors more effectively, all factors with *p* < 0.05 in univariate analyses were entered in a Cox proportional hazards model for multivariate survival analysis. When the effect of covariates was adjusted, *BRAF* mutation and increased PDL1 expression were independent predictors of poor DFS (HR = 2.38, 95% CI 1.02–5.56, *p* = 0.044; HR = 3.06, 95% CI 1.14–7.14, *p* = 0.025) (Table 4). In addition, risk category significantly influenced the probability of poor outcome (HR = 4.17, 95% CI 1.45–9.56, *p* = 0.009). Receiver operating characteristic (ROC) curve was used to determine discrimination and superiority of *BRAF* V600E, PDL1 and risk category. The area under the ROC curve was determined from the plot of sensitivity versus (1-specificity) [true positive rate versus false positive rate] and is a measure of the predictability of a test. A larger area under the

ROC curve of 0.70 to 0.90 is considered superior discrimination, whereas a ROC value of 0.50 indicates no discrimination.<sup>12</sup> The ROC areas for *BRAF* V600E, PDL1, and risk category were 0.781, 0.824, and 0.754, respectively (Fig. 6). This result indicated that compared with *BRAF* V600E and risk category, PDL1 alone was an even superior predictor of DFS in LCH.

## Discussion

In this study, we confirmed the feasibility of the high-specificity monoclonal antibody VE1 for detecting *BRAF* V600E mutation in 36/97 (37.1%) retrospectively enrolled patients with LCH, although the 94.8% concordant IHC and Sanger sequencing results obtained were lower than that of a previous study.<sup>13</sup> We then assessed the association between *BRAF* status and the tumor immune microenvironment. To the best of our knowledge, this is the first study to demonstrate that *BRAF* V600E mutation is significantly correlated to PDL1 expression and FOXP3<sup>+</sup> Treg levels in LCH. Notably, we found that *BRAF* mutation status and PDL1 were independent negative prognostic factors for DFS. Moreover, PDL1 showed a much better dis-

**Table 4.** Univariate and multivariate DFS analysis of prognostic factors for LCH (n = 97).

Variable	DFS		<i>p</i> value	HR	95%CI	<i>p</i> value
	Univariate analysis	Multivariate analysis				
	HR	95%CI				
Age (<18 y versus ≥18 y)	1.71	0.79–3.69	0.17			
Sex (male versus female)	1.34	0.62–2.91	0.46			
System (single versus multiple )	4.17	1.69–11.1	0.002**	1.09	0.41–3.57	0.473
Risk category (low versus high)	8.33	3.13–13.7	< 0.001***	4.17	1.45–9.56	0.009**
<i>BRAF</i> (wt versus mut)	2.71	1.23–5.92	0.013*	2.38	1.02–5.56	0.044*
G/T ratio (low versus high) <sup>a</sup>	1.06	0.48–2.34	0.88			
FOXP3 <sup>+</sup> Tregs (low versus high) <sup>a</sup>	2.43	1.02–6.25	0.046*	1.19	0.74–2.13	0.281
PDL1 (negative versus positive) <sup>b</sup>	3.45	1.39–8.33	0.007**	3.06	1.14–7.14	0.025*

\**p* < 0.05; \*\**p* < 0.01; \*\*\**p* < 0.001.

<sup>a</sup>Using median values as cut-off;

<sup>b</sup>Staining intensity ≥ 2 in >5% of LCH cells.



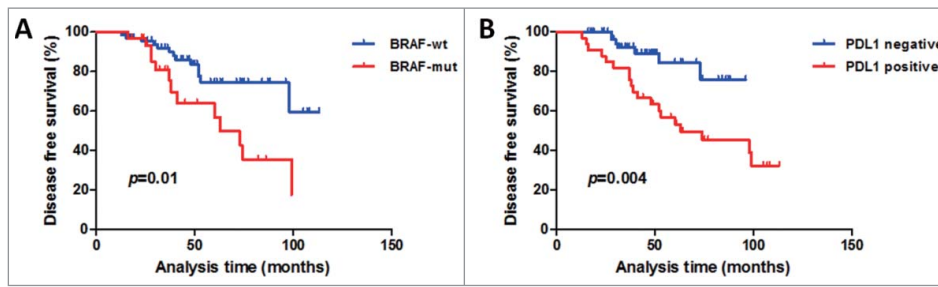


**Figure 5.** Kaplan–Meier DFS curves according to *BRAF* status and PDL1 expression in the 97-patient LCH cohort. (A) Patients with *BRAF* mutation had lower DFS rates than patients with wild-type *BRAF* did ( $p = 0.01$ ). (B) Patients with PDL1-positive expression had lower DFS rates than patients with PDL1-negative expression did ( $p = 0.004$ ). The log-rank test was used to determine the association between *BRAF* status and PDL1 expression and DFS, and the Kaplan–Meier method was used to generate survival curves. All tests were two-sided. wt = wild-type; mut = mutated.

crimination than *BRAF* V600E and risk category when the sensitivity and specificity were identified by ROC curves.

A breakthrough in understanding of the LCH pathogenesis came with the discovery<sup>4</sup> and validation<sup>13,14</sup> of recurrent *BRAF* V600E mutations in over 50% of LCH lesions. *BRAF* is a central kinase of the RAS–RAF–mitogen-activated protein kinase (MAPK) pathway, the involvement of which is essential in numerous cell functions, including cell proliferation and migration, and it is frequently mutated in various cancer cells.<sup>15</sup> In particular, emerging evidence suggests that the oncogenic *BRAF* contributes to immune evasion and that targeting this mutation may increase melanoma immunogenicity.<sup>16</sup> Consistent with a recent study,<sup>9</sup> we found that patients with *BRAF* V600E mutation LCH have high levels of FOXP3<sup>+</sup> Tregs more often as compared to *BRAF*-wt patients. Tregs are an immune-suppressive subpopulation of tumor-infiltrating lymphocytes (TIL) that reduce the activation of conventional T cells that

express the transcription factor FOXP3.<sup>17</sup> Moreover, increased FOXP3<sup>+</sup> Tregs in most tumors is associated with poor prognosis.<sup>18</sup> However, in our study, high FOXP3<sup>+</sup> Treg levels were only associated with poor DFS in univariate survival analysis ( $p = 0.046$ ), and there was no correlation in multivariate survival analysis ( $p = 0.281$ ).

Another important immune-suppressive factor, PDL1 (also called B7-H1 or CD274) has been implicated in tumor immune escape from the host immune system and in mediating tumor anti-apoptotic activity by binding programmed death-1 (PD-1) on activated cancer-specific T cells.<sup>19</sup> Recent studies have demonstrated that PDL1 is expressed in several tumor types, including melanoma, ovary, colon, lung, breast, and renal cell carcinoma; moreover, higher levels of PDL1 expression on tumors correlate with poor prognosis.<sup>20,21</sup> However, PDL1 expression has never been studied in LCH. In the present report, *BRAF* mutation was correlated with higher levels of PDL1 expression. Accumulating evidence shows that increased PDL1 expression is frequently found in many human cancer types, being upregulated in tumors by activation of key oncogenic pathways such as the class A phosphoinositide 3-kinases (PI3KCA)–AKT and RAS–RAF–MAPK pathways.<sup>22</sup> Moreover, Angell et al. showed that the *BRAF* V600E mutation was significantly associated with increased PDL1 expression in papillary thyroid cancer.<sup>10</sup> Consistently, a recent study demonstrated frequently high levels of PDL1 expression in systemic histiocytosis and showed that both PDL1 and *BRAF* V600E proteins colocalized to the same multinucleated LC.<sup>23</sup> Furthermore, we found that *BRAF* V600E mutation and PDL1 were independent prognostic factors of poor DFS in LCH via multivariate survival analysis.

Another interesting finding was the evidence that the G/T ratio could distinguish between clinical MS/SS multifocal and SS unifocal LCH. T-bet and GATA3 are Th1- and Th2-specific transcription factors, respectively, controlling Th1 or Th2 differentiation and overriding previously programmed cytokine patterns.<sup>24</sup> Immune balance controlled by Th1 and Th2 cells is critical for protecting the host against pathogenic invasion, while imbalance becomes the cause of various immune disorders. We found predominant Th2 over Th1 lymphoid infiltrate in the LCH tissues, and the mean G/T ratios were significantly higher in MS LCH and SS multifocal LCH as compared with SS unifocal LCH. The increase of Th2 levels accelerates the secretion of

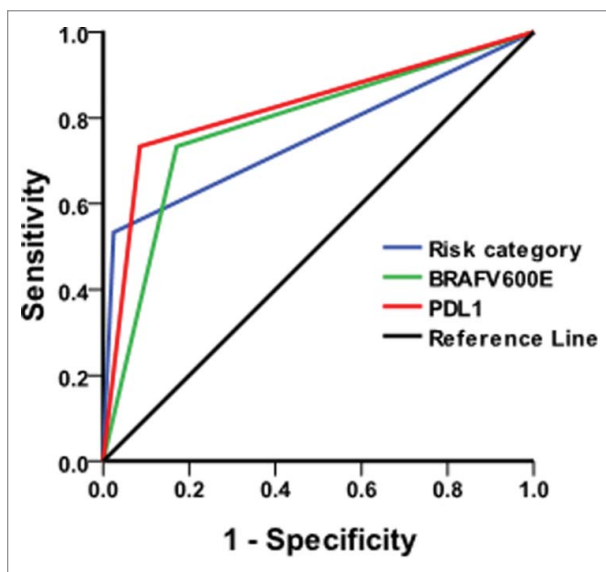


**Figure 6.** ROC curves of *BRAF* V600E, PDL1, and risk category. The area under the receiver operating characteristic (ROC) curve is a measure of the predictability of a test and was determined from the plot of sensitivity versus (1-specificity) [true positive rate versus false positive rate]. An area under the ROC curve of 0.7 to 0.9 is considered excellent discrimination, whereas a ROC value of 0.5 indicates no discrimination. When a test has strong discrimination value, the ROC curve will move up to the upper left-hand corner and the area under the curve will be close to 1.0. The ROC areas for *BRAF* V600E, PDL1, and risk category were 0.781, 0.824, and 0.754, respectively.

interleukin (IL)-10 and IL-4 and inhibits cellular immune function.<sup>25</sup> In a recent study, Monte et al. showed that the G/T ratio of tumor-infiltrating lymphoid cells is an independent negative predictive marker of survival.<sup>26</sup> However, in our study, the Cox regression model showed no significant correlation between the G/T ratio and LCH survival. Future studies will address the mechanisms by which Th2 cells promote tumor progression, and specifically, which cellular and molecular interactions they use to do so within the tumor immune microenvironment.

This work should be considered in light of a number of limitations. The major weakness of our study is that it includes only retrospectively collected samples and information. The retrospective nature of the collection is associated with potential bias from variable treatments.

Targeted therapy against oncogenic *BRAF* V600E mutation represents one of the most significant advances in melanoma treatment in decades. Recent studies have shown that the *BRAF* inhibitor vemurafenib is very effective against LCH with *BRAF* V600E mutation.<sup>27</sup> However, responses to vemurafenib are not durable, with a median time to progression of less than 6 mo. Consequently, strategies to increase the durability of these responses are urgently needed. Fortunately, the recent breakthroughs brought about by the clinical use of immune checkpoint inhibition in cancer excitingly promise long-term responses in clinically significant numbers of patients.<sup>28</sup> For example, clinical trials with monoclonal antibodies targeting PD-1 and PDL1 have shown promising response rates (30%–50%), with activity in melanoma and other cancers such as renal cell carcinoma and non-small cell lung cancer.<sup>29</sup> Moreover, increased T cell exhaustion markers, including TIM3, PD-1, and PDL1, were noted in tumor samples from patients treated with *BRAF* inhibitors, suggesting a potential resistance mechanism.<sup>30</sup> Notably, combining immunotherapy and *BRAF* targeted therapy might result in improved antitumor activity with high response rates of targeted therapy and durability of responses with immunotherapy in *BRAF* V600E mutant melanoma.<sup>31</sup>

In summary, our study identifies for the first time in LCH relationship between *BRAF* V600E mutation and PDL1 expression and FOXP3<sup>+</sup> Tregs, resulting in disruption of host–tumor immune surveillance, which is associated with reduced DFS. Our findings may provide a rationale for combining immunotherapy and *BRAF* targeted therapy for treating *BRAF* V600E mutant LCH.

## Materials and methods

### Patient characteristics

The study cohort comprised 97 patients diagnosed with LCH at Xijing Hospital from 2006 to 2015. The patient characteristics were showed in Table S1. All patients were followed-up after surgery until December 31, 2015, with detailed and complete clinicopathological data. The follow-up time ranged 13–113 mo, with a median time of 44 mo. At the end of the follow-up period, 93 patients were still alive and four had died of the disease. The study was approved by the local ethics

committee, and informed consent was obtained from all patients before the study.

### PCR and sanger sequencing

DNA was extracted from paraffin-embedded LCH tissue samples using a QIAamp DNA FFPE tissue kit (QIAGEN #56404) according to the instructions. *BRAF* exon 15 was amplified by PCR with the following primers: Forward 1: 5'-TAAACTCTT-CATAATGCTTGCTCTGAT-3', Forward 2: 5'-CATAATGCTTGCTCTGATAGGAAAATGAG-3'; and Reverse: 5'-AACT-CAGCAGCATCTCAGGGCCAA-3'. PCR was performed on PCR System 9700 (ABI). The *BRAF* gene was amplified by nested PCR with the following cycling conditions: in the first-round PCR, the total volume was 25  $\mu$ L: initial denaturation at 95°C for 10 min, followed by 40 cycles with denaturation at 95°C for 30 s, annealing at 60°C for 30 s, extension at 72°C for 30 s, and final extension at 72°C for 10 min. The second-round PCR was same as the first but the total volume was 50  $\mu$ L. Negative controls were included in each set of amplifications. PCR products were detected by 1.5% agarose gel electrophoresis, purified and sequenced using a Big Dye Terminator kit (Applied Biosystems), and analyzed on an ABI 3730XL DNA Analyzer (Applied Biosystems). Chromas software was used to analyze the sequencing results.

### Immunohistochemistry

IHC was performed on formalin-fixed, paraffin-embedded tissue sections. Serial sections (5- $\mu$ m thick) were dewaxed and rehydrated. Heat-induced antigen retrieval was followed by endogenous peroxidase activity blockade with hydrogen peroxide. The sections were incubated overnight at 4°C with the following primary antibodies: CD207 (1:50; Atlas Antibodies), VE1 (1:50; Spring Bioscience), FOXP3 (1:75; Abcam), and PDL1 (1:50; R&D Systems). For antigen visualization, a peroxidase-labeled secondary antibody (EnVision/HRP system; DAKO) was used. Subsequently, the sections were rinsed in the kit buffer and immersed in diaminobenzidine stain. The expression of GATA3 (1:100; Cell Signaling Technology) and T-bet (1:50; Abcam) was performed via double IHC staining using DouMaxVision immunohistochemical double dye kits (KIT-9998; Maixin Biotech) according to the manufacturer's instructions, with 5-bromo-4-chloro-3-indolyl phosphate/nitroblue tetrazolium as the blue-black chromogen for alkaline phosphatase and 3-amino-9-ethylcarbazole as the red chromogen for horseradish peroxidase. The sections were counterstained with Harris' hematoxylin and then mounted. For the negative controls, phosphate-buffered saline was used instead of primary antibody.

### Interpretation of IHC analyses

Two experienced pathologists examined the stained slides without any prior information on the clinicopathological features of the samples. The semiquantitative H-score approach was used.<sup>32</sup> Staining percentages (0–100%) and staining intensity of VE1 and PDL1 (0–3: 0, negative; 1, very weak; 2, moderate; 3, strong) in LCH cells and FOXP3<sup>+</sup> Tregs in TIL were evaluated

for each score, and the mean VE1, PDL1, and FOXP3<sup>+</sup> Treg scores were calculated (0–300) by multiplying the percentage of tumor area stained by the staining intensity. For GATA3 and T-bet evaluation, lymphocytes with nuclear staining were counted using the IHC Nuclear Image Analysis algorithm of Spectrum Plus software (Aperio) and normalized to a 1-mm<sup>2</sup> area. For FOXP3<sup>+</sup> Treg and G/T evaluation, the median value was used as the cut-off value as shown in the literature.<sup>26</sup> Furthermore, a tumor sample was considered PDL1-positive if 2+ intensity (complete membranous staining) was observed in ≥ 5% of cells.<sup>33</sup>

### Statistical analysis

Clinical characteristics and associations with biomarkers were examined by comparing the differences by chi-square test or Fisher's exact test as appropriate. Student's *t*-test and Pearson's correlation coefficients were used to evaluate correlations between *BRAF* mutation status and FOXP3<sup>+</sup> Tregs and PDL1 H-score values. DFS was calculated as the time from first LCH diagnosis to first recurrence or death. Patients with neither recurrence nor death at the end of the study were censored at the time of the last follow-up. Survival curves were estimated with the Kaplan–Meier method, and curves were compared with the log-rank test. Cox proportional hazards models were used for univariate and multivariate analyses. Results are expressed as HR with 95% CI. To determine discrimination, the sensitivity and specificity of the given data were identified as well, which were demonstrated using ROC curve. The significance level for all analyses was set at  $p < 0.05$  and all probability values were from two-sided tests. Statistical analysis was performed using IBM-SPSS Statistics version 20 (IBM Corp.). Figures were produced using GraphPad Prism 6.0 and Adobe Photoshop.

### Disclosure of potential conflicts of interest

No potential conflicts of interest were disclosed.

### Funding

This work was supported by the National Natural Science Foundation of China (No.81071951).

### References

- Willman CL, Busque L, Griffith BB, Favara BE, McClain KL, Duncan MH, Gilliland DG. Langerhans' cell histiocytosis (histiocytosis X)—a clonal proliferative disease. *N Engl J Med* 1994; 331:154–60; PMID:8008029; <http://dx.doi.org/10.1056/NEJM199407213310303>
- Broadbent V, Egeler RM, Nesbit MJ. Langerhans cell histiocytosis—clinical and epidemiological aspects. *Br J Cancer Suppl* 1994; 23:S11–6; PMID:8075001
- Arico M, Egeler RM. Clinical aspects of Langerhans cell histiocytosis. *Hematol Oncol Clin North Am* 1998; 12:247–58; PMID:9561898; [http://dx.doi.org/10.1016/S0889-8588\(05\)70508-6](http://dx.doi.org/10.1016/S0889-8588(05)70508-6)
- Badalian-Very G, Vergilio JA, Degar BA, MacConaill LE, Brandner B, Calicchio ML, Kuo FC, Ligon AH, Stevenson KE, Kehoe SM et al. Recurrent *BRAF* mutations in Langerhans cell histiocytosis. *Blood* 2010; 116:1919–23; PMID:20519626; <http://dx.doi.org/10.1182/blood-2010-04-279083>
- Bubolz AM, Weissinger SE, Stenzinger A, Arndt A, Steinestel K, Bruderlein S, Cario H, Lubatschowski A, Welke C, Anagnostopoulos I et al. Potential clinical implications of *BRAF* mutations in histiocytic proliferations. *Oncotarget* 2014; 5:4060–70; PMID:24938183; <http://dx.doi.org/10.18632/oncotarget.2061>
- Egeblad M, Nakasone ES, Werb Z. Tumors as organs: complex tissues that interface with the entire organism. *Dev Cell* 2010; 18:884–901; PMID:20627072; <http://dx.doi.org/10.1016/j.devcel.2010.05.012>
- Senechal B, Elain G, Jeziorski E, Grondin V, Patey-Mariaud DSN, Jaubert F, Beldjord K, Lellouch A, Glorion C, Zerah M et al. Expansion of regulatory T cells in patients with Langerhans cell histiocytosis. *Plos Med* 2007; 4:e253; PMID:17696642; <http://dx.doi.org/10.1371/journal.pmed.0040253>
- Coury F, Annels N, Rivollier A, Olsson S, Santoro A, Speziani C, Azocar O, Flacher M, Djebali S, Tebib J et al. Langerhans cell histiocytosis reveals a new IL-17A-dependent pathway of dendritic cell fusion. *Nat Med* 2008; 14:81–7; PMID:18157139; <http://dx.doi.org/10.1038/nm1694>
- Leslie C, Bowyer SE, White A, Grieu-Iacopetta F, Trevenen M, Iacopetta B, Amanuel B, Millward M. FOXP3<sup>+</sup> T regulatory lymphocytes in primary melanoma are associated with *BRAF* mutation but not with response to *BRAF* inhibitor. *Pathology* 2015; 47:557–63; PMID:26308130; <http://dx.doi.org/10.1097/PAT.0000000000000314>
- Angell TE, Lechner MG, Jang JK, Correa AJ, LoPresti JS, Epstein AL. *BRAF* V600E in papillary thyroid carcinoma is associated with increased programmed death ligand 1 expression and suppressive immune cell infiltration. *Thyroid* 2014; 24:1385–93; PMID:24955518; <http://dx.doi.org/10.1089/thy.2014.0134>
- Brown NA, Furtado LV, Betz BL, Kiel MJ, Weigelin HC, Lim MS, Elenitoba-Johnson KS. High prevalence of somatic *MAP2K1* mutations in *BRAF* V600E-negative Langerhans cell histiocytosis. *Blood* 2014; 124:1655–8; PMID:24982505; <http://dx.doi.org/10.1182/blood-2014-05-577361>
- Johann DJ, McGuigan MD, Patel AR, Tomov S, Ross S, Conrads TP, Veenstra TD, Fishman DA, Whiteley GR, Petricoin ER, Liotta LA. Clinical proteomics and biomarker discovery. *Ann N Y Acad Sci* 2004; 1022:295–305; PMID:15251975; <http://dx.doi.org/10.1196/annals.1318.045>
- Sahm F, Capper D, Preusser M, Meyer J, Stenzinger A, Lasitschka F, Berghoff AS, Habel A, Schneider M, Kulozik A et al. *BRAF*V600E mutant protein is expressed in cells of variable maturation in Langerhans cell histiocytosis. *Blood* 2012; 120:e28–34; PMID:22859608; <http://dx.doi.org/10.1182/blood-2012-06-429597>
- Berres ML, Lim KP, Peters T, Price J, Takizawa H, Salmon H, Idoyaga J, Ruzo A, Lupo PJ, Hicks MJ et al. *BRAF*-V600E expression in precursor versus differentiated dendritic cells defines clinically distinct LCH risk groups. *J Exp Med* 2014; 211:669–83; PMID:24638167; <http://dx.doi.org/10.1084/jem.20130977>
- Davies H, Bignell GR, Cox C, Stephens P, Edkins S, Clegg S, Teague J, Woffendin H, Garnett MJ, Bottomley W et al. Mutations of the *BRAF* gene in human cancer. *Nature* 2002; 417:949–54; PMID:12068308; <http://dx.doi.org/10.1038/nature00766>
- Sumimoto H, Imabayashi F, Iwata T, Kawakami Y. The *BRAF*-*MAPK* signaling pathway is essential for cancer-immune evasion in human melanoma cells. *J Exp Med* 2006; 203:1651–6; PMID:16801397; <http://dx.doi.org/10.1084/jem.20051848>
- Sakaguchi S, Miyara M, Costantino CM, Hafler DA. FOXP3<sup>+</sup> regulatory T cells in the human immune system. *Nat Rev Immunol* 2010; 10:490–500; PMID:20559327; <http://dx.doi.org/10.1038/nri2785>
- Gerber AL, Munst A, Schlapbach C, Shafiqhi M, Kiermeir D, Husler R, Hunger RE. High expression of FOXP3 in primary melanoma is associated with tumour progression. *Br J Dermatol* 2014; 170:103–9; PMID:24116716; <http://dx.doi.org/10.1111/bjd.12641>
- Iwai Y, Ishida M, Tanaka Y, Okazaki T, Honjo T, Minato N. Involvement of PD-L1 on tumor cells in the escape from host immune system and tumor immunotherapy by PD-L1 blockade. *Proc Natl Acad Sci U S A* 2002; 99:12293–7; PMID:12218188; <http://dx.doi.org/10.1073/pnas.192461099>
- Thompson RH, Kuntz SM, Leibovich BC, Dong H, Lohse CM, Webster WS, Sengupta S, Frank I, Parker AS, Zincke H et al. Tumor B7-



- H1 is associated with poor prognosis in renal cell carcinoma patients with long-term follow-up. *Cancer Res* 2006; 66:3381-5; PMID:16585157; <http://dx.doi.org/10.1158/0008-5472.CAN-05-4303>
21. Dong H, Strome SE, Salomao DR, Tamura H, Hirano F, Flies DB, Roche PC, Lu J, Zhu G, Tamada K et al. Tumor-associated B7-H1 promotes T-cell apoptosis: a potential mechanism of immune evasion. *Nat Med* 2002; 8:793-800; PMID:12091876; <http://dx.doi.org/10.1038/nm0902-1039c>
  22. Parsa AT, Waldron JS, Panner A, Crane CA, Parney IF, Barry JJ, Cachola KE, Murray JC, Tihan T, Jensen MC et al. Loss of tumor suppressor PTEN function increases B7-H1 expression and immunoresistance in glioma. *Nat Med* 2007; 13:84-8; PMID:17159987; <http://dx.doi.org/10.1038/nm1517>
  23. Gatalica Z, Bilalovic N, Palazzo JP, Bender RP, Swensen J, Millis SZ, Vranic S, Von Hoff D, Arceci RJ. Disseminated histiocytoses biomarkers beyond BRAFV600E: frequent expression of PD-L1. *Oncotarget* 2015; 6:19819-25; PMID:26110571; <http://dx.doi.org/10.18632/oncotarget.4378>
  24. Zhu J, Yamane H, Cote-Sierra J, Guo L, Paul WE. GATA-3 promotes Th2 responses through three different mechanisms: induction of Th2 cytokine production, selective growth of Th2 cells and inhibition of Th1 cell-specific factors. *Cell Res* 2006; 16:3-10; PMID:16467870; <http://dx.doi.org/10.1038/sj.cr.7310002>
  25. Michel G, Mirmohammadsadegh A, Olasz E, Jarzebska-Deussen B, Muschen A, Kemeny L, Abts HF, Ruzicka T. Demonstration and functional analysis of IL-10 receptors in human epidermal cells: decreased expression in psoriatic skin, down-modulation by IL-8, and up-regulation by an antipsoriatic glucocorticosteroid in normal cultured keratinocytes. *J Immunol* 1997; 159:6291-7; PMID:9550434
  26. De Monte L, Reni M, Tassi E, Clavenna D, Papa I, Recalde H, Braga M, Di Carlo V, Doglioni C, Protti MP. Intratumor T helper type 2 cell infiltrate correlates with cancer-associated fibroblast thymic stromal lymphopoietin production and reduced survival in pancreatic cancer. *J Exp Med* 2011; 208:469-78; PMID:21339327; <http://dx.doi.org/10.1084/jem.20101876>
  27. Hyman DM, Puzanov I, Subbiah V, Faris JE, Chau I, Blay JY, Wolf J, Raje NS, Diamond EL, Hollebecque A et al. Vemurafenib in Multiple Nonmelanoma Cancers with BRAF V600 Mutations. *N Engl J Med* 2015; 373:726-36; PMID:26287849; <http://dx.doi.org/10.1056/NEJMoa1502309>
  28. Hamid O, Robert C, Daud A, Hodi FS, Hwu WJ, Kefford R, Wolchok JD, Hersey P, Joseph RW, Weber JS et al. Safety and tumor responses with lambrolizumab (anti-PD-1) in melanoma. *N Engl J Med* 2013; 369:134-44; PMID:23724846; <http://dx.doi.org/10.1056/NEJMoa1305133>
  29. Brahmer JR, Tykodi SS, Chow LQ, Hwu WJ, Topalian SL, Hwu P, Drake CG, Camacho LH, Kauh J, Odunsi K et al. Safety and activity of anti-PD-L1 antibody in patients with advanced cancer. *N Engl J Med* 2012; 366:2455-65; PMID:22658128; <http://dx.doi.org/10.1056/NEJMoa1200694>
  30. Frederick DT, Piris A, Cogdill AP, Cooper ZA, Lezcano C, Ferrone CR, Mitra D, Boni A, Newton LP, Liu C et al. BRAF inhibition is associated with enhanced melanoma antigen expression and a more favorable tumor microenvironment in patients with metastatic melanoma. *Clin Cancer Res* 2013; 19:1225-31; PMID:23307859; <http://dx.doi.org/10.1158/1078-0432.CCR-12-1630>
  31. Hu-Lieskovan S, Mok S, Homet MB, Tsoi J, Robert L, Goedert L, Pinheiro EM, Koya RC, Graeber TG, Comin-Anduix B et al. Improved antitumor activity of immunotherapy with BRAF and MEK inhibitors in BRAF(V600E) melanoma. *Sci Transl Med* 2015; 7:241r-279r; PMID:25787767; <http://dx.doi.org/10.1126/scitranslmed.aaa4691>
  32. Azim HJ, Peccatori FA, Brohee S, Branstetter D, Loi S, Viale G, Piccart M, Dougall WC, Pruneri G, Sotiriou C. RANK-ligand (RANKL) expression in young breast cancer patients and during pregnancy. *Breast Cancer Res* 2015; 17:24; PMID:25849336; <http://dx.doi.org/10.1186/s13058-015-0538-7>
  33. Herbst RS, Soria JC, Kowanetz M, Fine GD, Hamid O, Gordon MS, Sosman JA, McDermott DF, Powderly JD, Gettinger SN et al. Predictive correlates of response to the anti-PD-L1 antibody MPDL3280A in cancer patients. *Nature* 2014; 515:563-7; PMID:25428504; <http://dx.doi.org/10.1038/nature14011>